Chapter to appear in “Animal Models of Acute Neurological Injuries" (Jun Chen, Zao Xu, Xiao-Ming Xu and John Zhang, editors), 2007, Contemporary Neuroscience Series, The Humana Press Inc.

Targeted occlusion to surface and deep vessels in neocortex via linear and nonlinear optical absorption

David Kleinfeld, Ph.D.[1,2], Beth Friedman, Ph.D.[3], Patrick D. Lyden, M. D. [2,3] and Andy Y. Shih, Ph.D.[1]

[1]Department of Physics
[2]Graduate Program in Neurosciences
[3]Department of Neuroscience
University of California at San Diego
La Jolla, CA 92093

Figures: 7 (5 in color)
Tables: 1
Narrative: 3,700 words
References 36

Running Title: Targeted occlusions

Key words: Ablation, Clot, Hypoxia, Ischemia, Microstroke, Photosensitizer, Plasma, Rodent, Two-photon.

Correspondence: David Kleinfeld
Department of Physics 0374
University of California
9500 Gilman Drive
La Jolla, CA 92093
Office: 858-822-0342
Fax: 858-534-7697
Email: dk@physics.ucsd.edu

Summary

We discuss two complementary methods for the study of cerebral blood flow and brain function in response to the occlusion of individual, targeted blood vessels. These bear on the study of microstroke and vascular dysfunction in cortex. One method makes use of linear optical absorption by a photosensitizer, transiently circulated in the blood stream, to induce an occlusion in a surface or near-surface vessel. The second method makes use of nonlinear optical interactions, without the need to introduce an exogenous absorber, to induce an occlusion in a subsurface microvessel. A feature of both methods is that the dynamics of blood flow and functional aspects of the vasculature and underlying neurons in the neighborhood of the occluded vessel may be monitored before, during, and after the occlusion. We present details of both methods and associated surgical procedures, along with example data from published studies.

1. Introduction

There are several forms of vascular dysfunction that can contribute to the onset of blood flow disturbances and neurodegeneration[1]. We consider dysfunction that is caused by vessel occlusion, which leads to ischemia. Our focus is on techniques that can occlude individual, targeted single vessels. The importance of targeting is three-fold. First, it provides a means to select a particular type of vessel, *e.g.*, capillary versus surface artery. Second, It provides a means to select a vessel at a particular location, *e.g.*, within a selected cortical column. Lastly, it provides a means to make both pre- and post-measurements of hemodynamic and neuronal state variables in the region that neighbors the occluded vessel.

The diameter of vessels in neocortex range over an order of magnitude in size. Surface communicating arterioles, which form a supply network for the underlying parenchyma, span 20 to 50 μm in diameter, penetrating arterioles, which transfer blood from the surface to the parenchyma, span 10 to 25 μm in diameter, and the microvessels and capillaries that supply the parenchyma span 5 to 10 μm in diameter[2]. A variety of techniques have been developed to induce occlusions in all of these vessels (Table 1). One class of procedures involves the introduction of small particles to the blood stream, such as microspheres or small thrombo-emboli, that can be tailored to lodge in arterioles of a particular size and produce occlusions. However, the location of the occlusion cannot be targeted. A second class of procedures involves the local injection of a powerful vasoconstrictor, particularly endothelin-1, that can be targeted to specific arteries and arterioles but typically spreads within the extracellular space to impact many vessels rather than just the desired target. A final class makes use of physical blockages, including ligation by a fine suture or a fine cautery. This approach is appropriate for relatively large arteries and veins on the cortical surface. Our goal has been to exploit the physical localization of highly focused laser light to form occlusions.

We consider two complementary techniques to form occlusions, both of which require the concurrent use of *in vivo* confocal laser scanning microscopy or *in vivo* two-photon laser scanning microscopy (TPLSM) as a means to image the underlying vasculature

and select a vessel for a targeted occlusion. *In vivo* TPLSM is particularly advantageous as it allows fluorescently labeled structures to be visualized at depths of 500 to 1000 um below the cortical surface[3]. The first technique makes use of near-threshold optical activation of the photosensitizer Rose Bengal and is suitable for vessels at the surface of the brain[4, 5]. These include the communicating arteries and the initial segment of the penetrating arterioles that branch off of the communicating arteries. The second makes use of plasma-mediated ablation through the nonlinear absorption of 100-fs, ultrashort laser pulses by blood plasma or the vascular wall[6]. This technique is suitable for subsurface vessels, such as arterioles, capillaries, and venules, as vessels above and below the target vessel are unaffected. However, this technique appears not to be suitable for surface vessels, as the energy deposited can lead to rupture of the free surface.

2. Common Procedures

Our procedures are applicable to any laboratory animal, although the majority of our experiments to date involve the adult rat with an observation window placed over parietal cortex. The underlying vasculature is imaged with *in vivo* TPLSM[7], with contrast generated by labeling of the blood plasma with high molecular weight fluorescein isothiocyanate-conjugated dextran[8-10] (fluorescein-dextran) (2 MDa, Sigma) . Vessels throughout the cranial window are first mapped at low-magnification, typically 4-X (*e.g.*, UB950, Olympus), to form a single map of an area of the exposed cortex. Target vessels for photodisruption are typically selected using the criteria that a portion of the vessel courses parallel to the cortical surface. We then map the local vascular architecture in the vicinity of the target vessel with a three-dimensional stack of images at high-magnification, typically 40-X (*e.g.*, UM568, Olympus).

3. Photosensitizer-mediated occlusion of surface vessels

This technique involves the introduction of a photosensitizer, in our case Rose Bengal, into the blood stream and the subsequent irradiation of the target vessel with actinic light, green laser-light in our case (Fig. 1A). The intensity of the light is adjusted to be at the threshold for photo-thrombosis in the plane of the target surface vessel. Light that

propagates into the parenchyma will be lower in intensity and thus below the threshold level to induce photo-thrombotic damage. This allows formation of the occlusion that is restricted to the surface vessel based on three physical mechanisms: (1) absorption of the incident light by the target vessel; (2) divergence of the beam beyond the target vessel as a result of the strong focus; and (3) scattering of light by brain tissue. However, small thrombi may be formed during the period of illumination that travel downstream rather than stick at the site of the irradiated region.

The persistence of Rose Bengal within the blood plasma may be estimated from *in vivo* measurements of its fluorescence, which peaks near 580 nm (omlc.ogi.edu/spectra/PhotochemCAD/html/), in the plasma. In mouse, which has approximately a 10-fold smaller blood volume than rat, Rose Bengal is cleared from circulation within 5 minutes[11] (Fig. 2).

3.1. Equipment

Formation of an occlusion with a photosensitizer is readily combined with TPLSM to enable the targeting and real-time monitoring of blood vessels. The typical set-up makes use of a standard two-photon microscope, either home-built[12, 13] or a commercial instrument (*e.g.*, Ultima with optional high speed two-photon optics set and external detector; Prairie Technologies), in which a 20 mW or greater green (λ = 532 nm) laser light (*e.g.*, GCL-100-M, CrystaLaser) is introduced into the beam pathway with a dichroic mirror (Fig. 1B). We used a fixed location of the beam, centered along the optical axis. The diameter of the beam is typically adjusted to pass through a hole in the emission dichroic (2 in Fig. 1B) and underfills the back aperture of the objective. The final spot size is approximately 3 μm diameter and is brought to the same focus as the pulsed near-infrared beam for TPLSM using an appropriate telescope. In this case, the motorized/encoding X-Y stage can be used to reposition the animal to change the location of photoactivation. Alternatively, the green actinic light may be introduced through a second set of scanners so that the position may be shifted electromechanically (*e.g.*, Ultima with optional second-set of scanners). In all cases, the intensity of the laser light at the focus should initially be held at 0.1 mW, using a

tunable neutral density filter in the beam path, and increased as needed up to a maximum of 5 mW.

3.2 Procedure

1.) Prior to surgery:

a. Choice of anesthetic:

i. Isoflurane in a 30 % O_2 – 70 % N_2O gas mixture, *i.e.*, 4 % (v/v) induction and 1 to 2 % (v/v) maintenance, provides adjustable anesthesia and the option of animal recovery.

ii. Urethane provides long-lasting and stable anesthesia, *i.e.*, 1000 mg per kg rat initial dose with 100 mg per kg supplements as required, but is difficult to adjust and is inappropriate for recovery. When using urethane, a 30 % O_2 – 70 % N_2O gas mixture is delivered to maintain normal blood gas levels.

iii. Other anesthetic agents are also suitable for this procedure[14].

b. Check for lack of toe pinch reflex to ensure adequate level of anesthesia.

c. Secure animal in stereotaxic frame.

d. Inject atropine, 0.05 mg per kg rat, intraperitoneal (i.p.) to reduce respiratory distress.

e. Apply opthalamic ointment to eyes to retain moisture.

f. Inject 2 % (v/v) Lidocaine™ into the scalp subcutaneously before incision for local anesthesia.

2.) Throughout surgery and recording (Fig. 3D):

a. Ensure heart and breathing rates are within a normal range, *i.e.*, 300 to 400 and 60 to 120 events per minute, respectively, using a pulse oximeter (8600V; Nonin).

b. Maintain body temperature at 37°C using a feedback regulated rectal probe and heat pad (Harvard).

c. Inject (i.p.) saline with 5 % (w/v) dextrose, 3 mL per kg rat every 2 hours to maintain body fluids and energy requirements.

d. Install a femoral artery catheter to allow blood samples to be collected. Blood gas is monitored once every 2 hours (Rapid Lab 248; Bayer). The normal range is 80 to 100 mm Hg for pO_2, 35 to 45 mm Hg for pCO_2, and 7.35 to 7.45 for pH.

e. Monitor arterial blood pressure (XBP1000; Kent Scientific). The normal range is 80 to 130 mm Hg for systolic pressure and 60 to 100 mm Hg for diastolic pressure. We use tail-cuff device to measure blood pressure, but measurement through an intra-arterial catheter is also possible.

Note that fluctuations in physiological parameters, often caused by variation in the depth of anesthesia, can greatly influence cerebral blood flow. It is important to maintain these variables in a normal range and to take note of abrupt changes during the experiment.

3.) Surgery:

a. Generate a craniotomy above the brain region of interest using a high-speed drill (Fig. 3B). We typically consider measurements over primary somatosensory cortex, which is the part of parietal cortex that nominally lies between -1 and -5 mm relative to the Bregma point and between 1 and 7 mm from the midline on the medial-lateral axis[15].

b. Glue the metal frame to the skull with dental acrylic (Grip Cement; Dentsply). The frame rigidly holds the head of the animal to the optical apparatus (Figs. 3A and 3B). To achieve a reliable connection between acrylic and bone, the contact regions on the bone are cleaned of soft tissue, a thin layer of VetBond™ is applied, #000-3/32 self-tapping screws (Small Parts) are introduced to the anterior and posterior aspects of the skull, and screws, one of which passes through an opening in the frame, are then mechanically linked to the frame with dental acrylic (Figs. 3B).

c. Remove the dura after the dental acrylic has cured. It is crucial to avoid any bleeding, and thus not cut or tear across any large vessels in the dura. Removal of the dura greatly improves the optical field and is recommended.

d. Fill the interior of the chamber with 1.5 % (w/v) low melting point agarose (A-9793; Sigma) dissolved in artificial cerebral spinal fluid (ACSF) that contains neither carbonate nor phosphate which cause precipitation when the solution is boiled to dissolve the agarose[16] (Fig. 3B and 3C). The temperature of the agarose must not exceed approximately 37°C before it is applied to the brain.

e. Immediately seal the chamber using a cover glass as a window (Fig. 3C). With the addition of a cover glass, the frame serves to provide a chamber that seals and protects the cortex. Resealing the craniotomy is crucial for the suppression of excessive motion that otherwise ensues as a result of cranial-pressure fluctuations that are caused by heart beat and breathing[a].

f. Stabilize the animals on a platform for imaging, using the frame as a head support (Fig. 3D). We prepare a separate plate that can be transported between surgical and imaging suites with the animal and all physiological monitoring devices assembled as one unit.

g. Label the blood plasma with 2 MDa fluorescein-dextran through the femoral artery catheter as a means to generate contrast between the red blood cells (RBCs) and the plasma[b]. We inject a 1.0 mL per kg rat bolus of 5 % (w/v) solution of fluorescein-dextran in physiological saline. This high molecular weight dye provides stable labeling, typically 3 hours, and further acts to stain the damage in occluded vessels[4]. The dye is supplemented as needed.

4.) Imaging and occlusion:

a. Collect baseline vascular images at successive depths to construct a three dimensional stack of images for maximal projection or volume rendered

[a] The agarose between the cover glass and the cortex allows the cranial opening to be effectively resealed even if a narrow opening is left on the sides as a means to insert glass microelectrodes into cortex[7].

[b] The blood plasma may also be labeled through a tail-vein injection. Submerge the tail in warm water, *i.e.*, 37°C, for approximately 2 min and place a soft clamp at the base of the tail to dilate the veins. Starting as close to the tip of the tail as possible, insert a 24-gauge catheter and inject the bolus of fluorescein-dextran in physiological saline.

views of the vasculature. Flow parameters, such as the speed of RBCs, are derived from line-scan data (Fig. 4A). Structural parameters, such as the cross-section of vessels, are derived from planar scans.

b. Select a vessel to target for occlusion.
c. Inject a 1.0 mL per kg rat bolus of 1 % (w/v) solution of Rose Bengal in physiological saline through the catheter. Rose Bengal should be injected immediately prior to formation of the occlusion.
d. To initiate photo-thrombosis, aim the focal point of the green-light laser within the lumen of the target vessel but near the vessel wall. This will nucleate the clotting cascade and create an attachment point for the growing clot. The irradiation is periodically interrupted for brief epochs of imaging, typically 1 frame (0.2 s per frame) every 1 s for an 80 % duty cycle, so that formation of the clot can be observed in real time. If a clot does not occur close to the wall within 5 to 10 s of irradiation, increase the power by factors of two until clot begins to form.
e. Oscillate the relative position between the animal and the beam, at 0.1 to 0.5 Hz, to traverse the diameter of the blood vessel. Occlusion requires 10-300 s or irradiation. Larger vessels with relatively fast RBC flow, *i.e.*, surface vessels as opposed to penetrating arterioles, require more time to fully occlude; the exact time must be determined empirically.
f. A successful occlusion appears densely packed with immobile non-fluorescent RBCs often surrounded by a brighter region of stagnant fluorescent plasma (Figs. 1C, 4A, and 5A).
g. Collect post-occlusion measurements, as desired.
h. The hypoxia marker pimonidazole hydrochloride (Hypoxyprobe™; www.hypoxyprobe.com) forms stable protein-adducts in viable tissues with low oxygen content that can be detected by *post hoc* immunohistology. In particular, Hypoxyprobe™ can be used to locate relatively small zones of hypoxia caused by single vessel occlusions (Fig. 5B). We typically inject Hypoxyprobe™ intravenously (i.v.) just after occlusion and one hour before sacrifice.

5.) Histological examination.

a. It is often desirable to examine the consequences of single vessel occlusion using *post hoc* histology. The animal is trans-cardially perfused with saline followed by 4 % (w/v) paraformaldehyde in phophate buffered saline, the brain is removed, equilibrated with 30 % (w/v) sucrose, and frozen-sectioned. Extravasated fluorescein-dextran is trapped within the vessel wall at or near the site of the occlusion (Figs. 4B and 5B).

3.4 Example data

The pial arterioles of the cortical surface arteries form a communicating network, from which penetrating arterioles branch and dive to perfuse underlying capillary beds. In the first experiment, we selectively occluded a penetrating arteriole (yellow circle in Fig. 4A). Baseline and post-occlusion values of RBC velocities were measured in the target vessel, as well as neighboring microvessels, using continuous line-scans[17] of a segment of the vessel in the plane of the cortical surface. The location of the occlusion appeared as a bright region of stagnant serum within the vessel lumen and extravasated fluorescein-dextran indicated damage to the vessel wall. This occlusion was specific to the target vessel since the velocity of RBCs in a neighboring penetrating arteriole was unaffected (Vessel 1 in Fig. 4A). However, a downstream microvessel directly perfused by the target vessel experienced severe loss of blood flow (Vessel 2 in Fig. 4A). In a second animal, the hypoxic volume that resulted from the occlusion of a single penetrating arteriole was examined using *post hoc* histology (Fig. 4B). Immunostaining for Hypoxyprobe^{TM} revealed a column of hypoxic tissue that extended 700 μm beneath the pial surface. This result is consistent with the idea that penetrating arterioles, which are largely devoid of collateral flow, act as bottlenecks in the supply of blood to the cortex[5].

Occlusions placed within the redundant surface network[18] lead to a fundamentally different outcome. A typical example is shown in figure 5A, where a single vessel divides into downstream branches (1st frame). Green laser light was focused in the lumen of the main arteriole (yellow circle). In the absence of circulating Rose Bengal,

no occlusion was formed (2nd frame). However, immediately after injection of Rose Bengal, the irradiation initiates a clotting cascade against the vessel wall (3rd frame). Within 3 minutes of continuous irradiation, the vessel is completely occluded by a dense mass of clotted RBC with bright stagnant plasma directly upstream (5th frame). As with the example given above, surface vessels that neighbor the target vessel are not affected by photo-thrombosis, which demonstrates the specificity imparted by this technique.

One feature of disrupted flow in the surface arteriole network is the occurrence of robust flow reversals in downstream arterioles, which compensate for loss of flow caused by the occlusion. White arrows indicate baseline flow directions (Fig. 5A). Line-scans show that vessel 2 reverses after the occlusion, which allows the flow in vessels 1 and 3 to be maintained at near-baseline levels. *Post hoc* Hypoxyprobe™ staining revealed a much smaller hypoxic region compared to penetrating arteriole occlusion (Fig. 5B), showing that re-routing of blood flow offers protection against the formation of a large damage zone. A small field of fluorescein-dextran extravasation is still visible in the vicinity of the occlusion and overlaps with the hypoxic region. High-magnification views of Hypoxyprobe™ stained tissue reveals the staining of individual neurons (Fig. 5B).

4. Plasma-mediated occlusion of deep vessels

This technique makes use of the dissociation of matter by high-fluence, 100 to 300 fs pulses of near infrared light. These pulses lead to ionization of the material, such as blood plasma or vascular lumen, within a femtoliter-sized focal-volume of the incident laser pulse. The interaction of light towards the end of the pulse with the initial light-induced ionization results in a spatially-limited release of mechanical energy in the form of a shock wave (Fig. 6A). This method allows occlusions to be induced below the surface of cortex, typically down to 500 μm but in principle down to 1000 μm below the pia, without disruption of the neighboring tissue.

4.1. Equipment

Plasma-mediated occlusion is readily combined with TPLSM, as described above, to

enable the targeting and real-time monitoring of blood vessels. The typical set-up makes use of a standard two-photon microscope in which an amplified 100 fs light source is introduced to the beam path through a polarizing beam splitter (Fig. 6B). The imaging and photodisruption beams are focused to the same focal plane and the amplified beam is centered on the optical axis so that photodisruption occurred at the center of the imaged field. The energy per pulse of the photodisruption beam is varied with neutral density filters and the number of pulses is controlled by a mechanical shutter. There are multiple suppliers of "single-box" amplifiers, which consist of four devices in one housing, *i.e.*, a 100-fs Ti:Sapphire oscillator with associated pump to serve as the seed for the optical amplifier, together with a regenerative Ti:Sapphire-based amplifier and it's associated pump laser (*e.g.*, Libra, Coherent Inc.).

The diameter of the amplified 100-fs beam is adjusted to overfill the back aperture of the objective, using an appropriate telescope, to form the smallest possible spot size. The energy per pulse of the amplified beam should initially be set at 0.03 μJ, which corresponds to a near-threshold fluence for damage of approximately 1 J/cm^2 at the focus with a 40-X dipping objective, consistent with literature values for damage.

4.2. Procedure

The surgical and animal maintenance procedures are identical to those described for the photosensitizer-based occlusions. Similarly, histological examination of the tissue proceeds as described above. It is imperative to perform occlusions with concurrent imaging as a means to continuously monitor the state of the vasculature .

6.) Imaging and occlusion:

a. Collect baseline vascular images at successive depths to construct a three dimensional stack of images for maximal projection or volume rendered views of the vasculature (Fig. 6C). Flow parameters, such as the speed of RBCs, are derived from line-scan data. Structural parameters, such as the cross-section of vessels, are derived from planar scans.
b. Select a subsurface microvessel to target for occlusion.

c. Aim the focal point of the amplified 100 fs beam near the center of the lumen and irradiate for approximately 10 pulses at the minimum pulse energy. The first indication of photodisruption is visualized as the accumulation of fluorescein-dextran outside the vessel lumen; this corresponds to extravasation. If extravasation fails to occur, increase the energy by approximately a factor of 2 and irradiate again; extravasation typically occurs by 2- to 3-times times the threshold energy and in the range of 0.1 to 0.5 μJ per pulse.
d. Once extravasation occurs, the irradiation is repeated with increased pulse energy, typically by less than a factor of 2, and increasing number of pulses, typically 10 to 100, until there is a complete cessation of RBC movement in the target vessel. Increasing the energy further may result in the rupture of the vessel and a hemorrhage[c].
e. A successful occlusion appears densely packed with immobile non-fluorescent RBCs, abutted by a brighter region of stagnant fluorescent plasma. The occlusion is further delimited by the uptake of fluorescein-dextran in the endothelial cells of the vessels.

4.3. Example data

We consider a microvessel, approximately 10 μm in diameter, that lay approximately 250 μm below the pia (Fig. 7A). Uniform flow is seen in the vessel prior to irradiation, as evidenced by streaks in the raster-scanned imaged (panel 1 in Fig. 7A). Labeling of the vessel wall with trapped fluorescein-dextran is observed, but flow is still present, subsequent to the first burst of pulses (panels 2 and 3 in Fig. 7A). A second burst of pulses leads to cessation of flow and a stagnant pool of fluorescent plasma behind the occlusion (panels 4 and 5 in Fig. 7A). Lastly, measurements of the speed and direction of RBC flow before and after formation of the occlusion indicate that the occlusion effectively halts flow in vessels that lie immediately downstream (Fig. 7A).

[c] Preliminary findings suggest that irradiation of the wall of a penetrating arteriole with amplified 100-fs laser pulses, at a level deep to the surface, may be used to form an occlusion[19]. This builds on work that used unamplified pulses with subthreshold energies to irritate the vasculature[20], possibly by direct damage to RBCs through two-photon absorption of the incident 100-fs pulses[21].

A histological examination of a plasma-mediated occlusion in a different preparation shows that the hypoxia marker Hypoxyprobe™ stains tissue in a diffuse manner near the site of the occlusion (Fig. 7B). This staining is highly overlapped with the extravasated fluorescein-dextran in this section. Clotting activity is observed in the targeted vessel through anti-fibrin immunoreactivity, a marker of fibrin/fibrinogen clots. The fibrin forms a dense core deposit with a more diffuse surround that is highly overlapped with the extravasated fluorescein-dextran in the section (Fig. 7C).

5. Synopsis

We have described two methods that, collectively, allow occlusions to be targeted to single vessels that lie anywhere within the upper 500 to 1000 μm of cortex. These occlusions provide a means to address the consequences of vascular disease and microstrokes on a microscopic level. While past investigations have employed these relatively new methods to only acute studies, it is anticipated that the same occlusion and concurrent imaging techniques will be exploited for chronic investigations as well.

Acknowledgements

The authors are pleased to thank the Canadian Institutes of Health Research, the National Institutes of Health (NCRR, NIBIB and NINDS), the National Science Foundation, and the Veterans Medical Research Foundation for support.

Contact information

David Kleinfeld dk@ucsd.edu
Beth Friedman befriedman@ucsd.edu
Patrick D. Lyden plyden@ucsd.edu
Andy Y. Shih a2shih@ucsd.edu

References

1. Iadecola C. Neurovascular regulation in the normal brain and in Alzheimer's disease. Nature Reviews of Neuroscience 2004;5:347-60.
2. Scremin OU. Cerebral Vascular System. In: Paxinos G, ed. The Rat Nervous System. 2 ed. San Diego: Academic Press, Inc.; 1995.
3. Helmchen F, Denk W. Deep tissue two-photon microscopy. Nature Methods 2005;2:932-40.
4. Schaffer CB, Friedman B, Nishimura N, et al. Two-photon imaging of cortical surface microvessels reveals a robust redistribution in blood flow after vascular occlusion. Public Library of Science Biology 2006;4:258-70.
5. Nishimura B, Schaffer CB, Friedman B, Lyden PD, Kleinfeld D. Penetrating arterioles are a bottleneck in the perfusion of neocortex. Proceedings of the National Academy of Sciences USA 2007;104:365-70.
6. Nishimura N, Schaffer CB, Friedman B, Tsai PS, Lyden PD, Kleinfeld D. Targeted insult to individual subsurface cortical blood vessels using ultrashort laser pulses: Three models of stroke. Nature Methods 2006;3:99-108.
7. Svoboda K, Denk W, Kleinfeld D, Tank DW. *In vivo* dendritic calcium dynamics in neocortical pyramidal neurons. Nature 1997;385:161-5.
8. Kleinfeld D, Mitra PP, Helmchen F, Denk W. Fluctuations and stimulus-induced changes in blood flow observed in individual capillaries in layers 2 through 4 of rat neocortex. Proceedings of the National Academy of Sciences USA 1998;95:15741-6.
9. Kleinfeld D, Denk W. Two-photon imaging of neocortical microcirculation. In: Yuste R, Lanni F, Konnerth A, eds. Imaging Neurons: A Laboratory Manual. Cold Spring Harbor: Cold Spring Harbor Laboratory Press; 2000:23.1-.15.
10. Kleinfeld D, Denk W. Two-photon imaging of cortical microcirculation. In: Yuste R, Konnerth A, eds. Imaging In Neuroscience and Development. Cold Spring Harbor: Cold Spring Harbor Laboratory Press; 2005:701-5.
11. Zhang S, Murphy TH. Imaging the impact of cortical microcirculation on synaptic structure and sensory-evoked hemodynamic responses in vivo. Public Library of Science Biology 2007;5:e119.
12. Tsai PS, Nishimura N, Yoder EJ, Dolnick EM, White GA, Kleinfeld D. Principles, design, and construction of a two photon laser scanning microscope for *in vitro* and *in vivo* brain imaging. In: Frostig RD, ed. In Vivo Optical Imaging of Brain Function. Boca Raton: CRC Press; 2002:113-71.
13. Majewska A, Yiu G, Yuste R. A custom-made two-photon microscope and deconvolution system. Pflugers Archives 2000;441:398-408.
14. Short CE. Principles and Practice of Veterinary Anesthesia. Baltimore: Williams and Willisms; 1987.
15. Paxinos G, Watson C. The Rat Brain in Stereotaxic Coordinates. San Diego: Academic Press; 1986.
16. Kleinfeld D, Delaney KR. Distributed representation of vibrissa movement in the upper layers of somatosensory cortex revealed with voltage sensitive dyes. Journal of Comparative Neurology 1996;375:89-108.

17. Dirnagl U, Villringer A, Einhaupl KM. *In-vivo* confocal scanning laser microscopy of the cerebral microcirculation. Journal of Microscopy 1992;165:147-57.

18. Brozici M, van der Zwain A, Hillen B. Anatomy and functionality of leptomeningeal anastomoses: A review. Stroke 2003;34:2750-62.

19. Nishimura N, Rosidi NL, Mandell J, Iadecola C, Schaffer CB. Neighboring arterioles do not dilate to increase collateral flow after the occlusion of a cortical penetrating arteriole. In: Abstracts of the Society for Neuroscience Annual Meeting, Neuroscience 2007.

20. Nimmerjahn A, Kirchhoff F, Helmchen F. Resting microglial cells are highly dynamic surveillants of brain parenchyma in vivo. Science 2005;308(5726):1314-8.

21. Clay GO, Schaffer CB, Kleinfeld D. Large two-photon absorptivity of hemoglobin in the infrared range of 780 - 880 nm. Journal of Chemical Physics 2007;126:025102.

22. Miyake K, Takeo S, Kaijihara H. Sustained decrease in brain regional blood flow after microsphere embolism in rats. Stroke 1993;24:415-20.

23. Sugi T, Schuier FJ, Hossmann KA, Zulch KJ. The effect of mild microembolic injury on the energy metabolism of the cat brain. J Neurol 1980;223(4):285-92.

24. Gerriets T, Li F, Silva MD, et al. The macrosphere model: evaluation of a new stroke model for permanent middle cerebral artery occlusion in rats. J Neurosci Methods 2003;122(2):201-11.

25. Zhang Z, Zhang RL, Jiang Q, Raman SB, Cantwell L, Chopp M. A new rat model of thrombotic focal cerebral ischemia. J Cereb Blood Flow Metab 1997;17(2):123-35.

26. Fuxe K, Bjelke B, Andbjer B, Grahn H, Rimondini R, Agnati LF. Endothelin-1 induced lesions of the frontoparietal cortex of the rat. A possible model of focal cortical ischemia. Neuroreport 1997;8(11):2623-9.

27. Macrae IM, Robinson MJ, Graham DI, Reid JL, McCulloch J. Endothelin-1-induced reductions in cerebral blood flow: dose dependency, time course, and neuropathological consequences. J Cereb Blood Flow Metab 1993;13(2):276-84.

28. Sharkey J, Ritchie IM, Kelly PA. Perivascular microapplication of endothelin-1: a new model of focal cerebral ischaemia in the rat. J Cereb Blood Flow Metab 1993;13(5):865-71.

29. Zhang S, Boyd J, Delaney KR, Murphy TH. Rapid reversible changes in dendritic spine structure *in vivo* gated by the degree of ischemia. Journal of Neuroscience 2005;25:5333-228.

30. Wei L, Rovainen CM, Woolsey TA. Ministrokes in rat barrel cortex. Stroke 1995;26:1459-62.

31. Chen ST, Hsu CY, Hogan EL, Maricq H, Balentine JD. A model of focal ischemic stroke in the rat: Reproducible extensive cortical infarction. Stroke 1986;17(4):738-43.

32. Buchan AM, Xue D, Slivka A. A new model of temporary focal neocortical ischemia in the rat. Stroke 1992;23(2):273-9.

33. Tamura A, Asano T, Sano K. Corrrelation between rCBF and histological changes following temporary middle cerebral artery occlusion. Stroke 1980;11:487-93.

34. Katsman D, Zheng J, Spinelli K, Carmichael ST. Tissue microenvironments within functional cortical subdivisions adjacent to focal stroke. J Cereb Blood Flow Metab 2003;23(9):997-1009.

35. Markgraf CG, Kraydieh S, Prado R, Watson BD, Dietrich WD, Ginsberg MD. Comparative histopathologic consequences of photothrombotic occlusion of the distal middle cerebral artery in Sprague-Dawley and Wistar rats. Stroke 1993;24:286-93.

Table 1. Methods for occlusion of individual small vessels in cortex

Method	Vessel(s)	Targeted	Reperfusion	Representative References
Intravascular injection of microspheres (25-50 μm diameter)	Arterioles	No	No	22, 23
Intravascular injection of macrospheres (300-400 μm diameter)	Arteries	No	No	24
Intravascular injection of thrombo-emboli	Arteries Arterioles	No	Yes	25
Focal injection of vasoconstrictor (endothelin-1)	Arteries Arterioles	Partially	Yes	26-29
Suture ligation Micro-clip	Surface arteries	Yes	Yes	30-32
Thermo-coagulation Electro-coagulation	Surface arteries	Yes	No	33, 34
Photosensitizer (Rose Bengal)	Surface arteries Penetrating arterioles	Yes	Incompletely tested	4, 5, 29, 35
Plasma-mediated ablation (amplified 100 fs pulses)	Subsurface microvessels	Yes	No	5

Figure Legends

Figure 1. Overview for forming intravascular occlusions in surface vessels using focal illumination of Rose Bengal. (A) Green laser light is tightly focused through an objective and directed into the lumen of a target vessel. The circulating Rose Bengal dye is photo-activated and initiates a clotting cascade. **(B)** Schematic of a two-photon laser scanning microscope system modified to include a continuous wave (CW) green-light laser for photo-thrombosis. The green laser is directed onto the optical axis of the near-infrared beam with dichroic mirror 1 (625 DRLP; Chroma). An approximately 3.5-mm hole was etched in the coating of dichroic mirror 2 (700 DCXRU; Chroma) to allow transmission of the green laser beam; this results in at most a 10 % loss in collection efficiency. CW = continuous wave, ND = neutral density filter. **(C)** X-Z maximal projection of TPLSM image stack showing a penetrating arteriole selectively occluded by photo-thrombosis. All panels adapted from Schaffer *et al.*[4].

Figure 2. Time-scale for Rose Bengal clearance from circulation. Rose Bengal fluorescence in a cerebral arteriole was repeatedly measured after tail vein injection using TPLSM planar scans. Rose Bengal is largely cleared from circulation within 5 min. Data was collected from mouse, courtesy of Zhang and Murphy[11].

Figure 3. Methods for *in vivo* imaging of blood flow through a cranial window. (A) To immobilize the head of the animal during imaging, we designed a metal frame that could be cemented to the skull, and then anchored to an optical set-up. The frame is constructed of type 410 stainless steel with dimensions of 2.00 in long, 0.61 in wide and 0.029 in thick, and can be secured between two posts in a standard optical breadboard. An inset region, 0.015 in deep, borders the frame window to hold a cover glass over the craniotomy. The window cover, 0.015 in thick type 301 stainless steel, is then secured to the frame with four screws, sandwiching the no. 1 cover glass in place. **(B)** Surgical procedure for acute imaging experiments. The animal is placed in a stereotaxic frame. Lidocaine™ is subcutaneously injected into the scalp for local anesthesia. An approximately 5 cm midline incision is made in the scalp, and the periostium is scraped to the sides with a bone curette. The scalp is retracted using hemostats. The right temporalis muscle is separated from the bone, without severing, and retracted. The skull surface is cleaned with cotton swabs and bleeding from the skull is controlled with maintained pressure from the swab, or superficial abrasion with a high-speed drill. A thin layer of VetBond™, is applied to the skull surface to aid attachment of the dental acrylic and frame. The location of the cranial window is marked in pencil. We typically place

the window above the somatosensory cortex by centering a 4 x 4 mm craniotomy at -3.0 mm anterior-posterior and +4.5 mm medial-lateral. The edges of the marked cranial window are slowly thinned with a high-speed drill. The bone is flushed regularly with physiological saline to avoid over-heating. Drilling is stopped just as the bone begins to crackle and cerebral spinal fluid begins to leak through. The resulting island of bone is gently lifted away horizontal to the skull surface using two forceps on opposite corners of the bone flap. The underlying dura is flushed with ACSF and bleeding is controlled with small pieces of Gelfoam™ soaked in ACSF and KimWipes™, twisted to a fine point with the fingers. The cranial window is kept moist with a piece of moist Gelfoam™. Two burr holes are made with a 1/4 bit, anterior and posterior to the intended frame placement, self-tapping #000-3/32 screws are placed in the burr holes, and the threads secured with a small dab of VetBond™. The metal frame is fixed tangentially to the clean, dry skull surface with dental acrylic. Extra dental acrylic is built up around the screws to provide further anchoring support. A small nick is made in the dura with a bent 27 gauge syringe needle. The dura is carefully teased apart with fine forceps (Dumont #5), starting at the nick, and reflected to one side of the cranial window. The interior of the window chamber is filled with 37^{o}C, 1.5 % (w/v) low-melting-point agarose, dissolved in a modified version of ACSF (125 mM NaCl, 10 mM glucose, 10 mM HEPES, 3.1 mM $CaCl_2$, 1.3 mM $MgCl_2$, pH 7.4). The chamber is immediately sealed using a cover glass (no.1, cut to size), and the window cover is secured over the cover glass with four screws. The skin is sutured together around the frame, and agarose is trailed around the cover glass to hold water for the dipping lens. **(C)** A cross-sectional view of the cranial window. The inset diagram shows an inverted coronal view of surface vessels and deep microvessels that are targeted for occlusion. **(D)** A typical experimental set-up used in our laboratory. The metal frame attached to the skull is immobilized between two anchoring posts inserted into an optical breadboard. Anesthesia is maintained with isoflurane in a 30 % O_2 - 70 % N_2O gas mixture. Blood pressure is measured with a tail cuff device. The femoral artery catheter is used to collect blood samples for blood gas measurements, and is also the delivery route for fluorescein-dextran and Rose Bengal. Heart rate and blood O_2 saturation is continuously monitored using a pulse oximeter, which is useful in the assessing the depth of anesthesia. Rat skull diagram in panel B adapted from Paxinos[15].

Figure 4. Photo-thrombotic occlusion of penetrating arterioles using Rose Bengal. (A) Projected TPLSM image of a single penetrating arteriole occluded by photo-thrombosis (yellow circle) shown in the coronal plane (X-Z maximal projection), with surface arterioles near the top of the image. For the same field of interest, the surface vascular network is visible in the plane

tangential to the cortical surface (X-Y maximal projection). The velocity of RBCs in two neighboring surface vessels (Vessel 1 and 2) was measured using repeated line-scans. Vessel 1 shows no change in post-occlusion RBC velocity (v_{post}) compared to baseline (v_{base}), whereas Vessel 2 shows essentially no flow after the occlusion. **(B)** Examination of the hypoxic volume generated after a single penetrating arteriole was occluded (yellow cross). Hypoxyprobe™ was injected (i.v.) after clot formation and 1 h before sacrifice. The animal was trans-cardially perfused with 100 mL of saline followed by 100 mL of 4 % (w/v) paraformaldehyde. To locate the occluded vessel after brain extraction, fiducials markers were electrolytically placed near the target vessel before the brain was extracted from the skull. The entire ipsilateral cortex was removed and sandwiched between two glass slides separated by a distance of 2.5 mm. The tissue was post-fixed for 24 h, equilibrated with 30 % (w/v) sucrose, and sectioned on a freezing-sliding microtome into 100-μm sections tangential to the cortical surface. Immunostaining for Hypoxyprobe™ revealed a column of hypoxia, within the dashed yellow circles, that reached 700 μm below the pial surface. Panel A adapted from Nishimura *et al.*[5].

Figure 5. Photo-thrombotic occlusion of surface arterioles using Rose Bengal. (A) Planar TPLSM images showing the time-course for photo-thrombotic occlusion of a single surface arteriole. The 1st frame was taken at baseline, and white arrows indicate the directions of RBC flow as determined by line-scans. Three vessels branching from the main arteriole, numbered 1 to 3, were examined for flow direction and RBC velocity before and after the occlusion. In the 2nd frame, the yellow circle indicates the location of green laser irradiation. In the absence of circulating Rose Bengal, a 2-min period of irradiation did not form a clot. After the intravenous injection of Rose Bengal, irradiation initiated clot formation within 2 min and completely occluded the target vessel by 3 min. Surrounding vessels were unaffected by targeted photo-thrombosis. The occlusion appears as a dark mass of clotted RBCs with brightly fluorescent blood plasma directly upstream from the occlusion. Linescans show that the occlusion resulted in a re-routing of flow in downstream vessels. Notably, a flow reversal occurred in vessel 2 allowing vessels 1 and 3 to maintain near baseline levels of RBC velocity. **(B)** Hypoxyprobe™ was injected (i.v) 1 h after occlusion. The animal was trans-cardially perfused and the brain was prepared for histology (Fig. 4). The brain was cryo-sectioned along the coronal plane and immuno-stained for Hypoxyprobe™. Hypoxia was restricted to a zone immediately beneath the site of occlusion. Lateral and medial directions are labeled by M and L, respectively. Below, a mixed brightfield-fluorescent image, plus fluorescence, shows that the extravasated fluorescein-

dextran overlaps with the hypoxic region. High-magnification images show specific Hypoxyprobe™ labeling of individual neurons. All panels adapted from Schaffer *et al.*[4].

Figure 6. Overview for forming intravascular occlusions in deep microvessels using amplified 100-fs laser pulses. (A) Laser pulses directed on a deep microvessel (top image) leads to a release of mechanical energy in the form of a shock wave (middle image). Repeated delivery of pulses, starting at low energies and gradually increasing, forms an occlusion within the target vessel (bottom image). **(B)** Schematic of a two-photon laser-scanning microscope system modified for delivery of amplified 100-fs pulses. The dichroic is a 700 DCXRU (Chroma). **(C)** A projected X-Z TPLSM image stack showing deep microvessels (yellow cross) that are routinely targeted for selective occlusion using this technique. All panels adapted from Nishimura *et al.*[6].

Figure 7. Example of targeted deep microvessel occlusion using amplified 100-fs laser pulses. (A) Maximal projection of a TPLSM stack showing a tortuous network of sub-surface microvessels. The second row shows planar images taken from a region of interest (white rectangle) depicting the time-course for intravascular clot formation (frames 1-5). The red pulses indicate irradiation with multiple trains of 0.03-µJ pulses delivered at 1 kHz. After the first pulse, there was temporary cessation of RBC motion and swelling of the target vessel (frames 2 and 3). A second pulse led to limited extravasation and finally occlusion of the vessel lumen (frames 4 and 5). The third row shows vascular traces with baseline and post-occlusion RBC velocity profiles, in mm/s, of the vascular network. Arrow-heads denote the direction of RBC movement and the red cross marks the occluded microvessel. **(B)** Immunolabeling of tissue after deep microvessel occlusion. The red ellipses delineate a common area in the vicinity of the occlusion. Diffuse Hypoxyprobe™ immunostaining overlaps with affected region surrounding the occlusion, as marked by the territory of fluorescein-dextran extravasation. **(C)** Anti-fibrin immunostaining reveals localization of fibrin/fibrinogen clots, which appears as a mixed diffuse zone that surrounds a small dense region of intense staining. A mixed brightfield-fluorescence image (plus fluorescence) shows that fibrin immunoreactivity is also confined to the immediate vicinity of the occlusion. All panels adapted from Nishimura *et al.*[6].

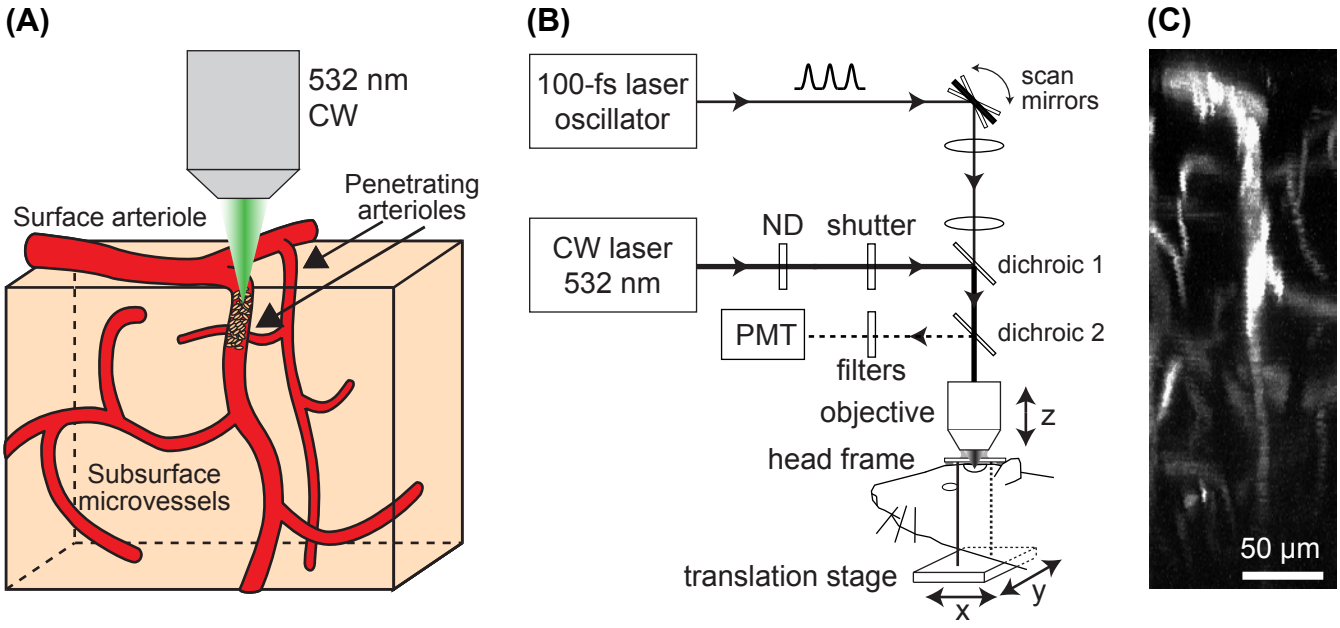

Figure 1. Kleinfeld, Friedman, Lyden and Shih

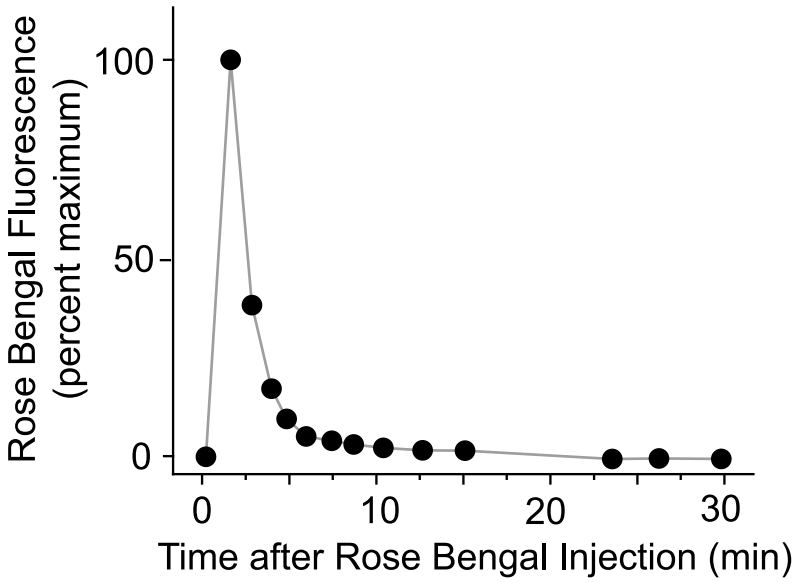

Figure 2. Kleinfeld, Friedman, Lyden and Shih

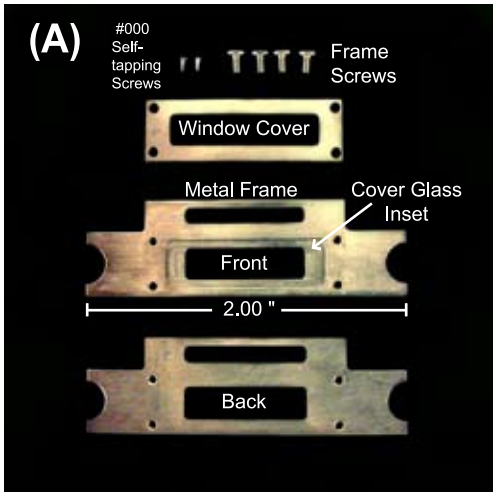

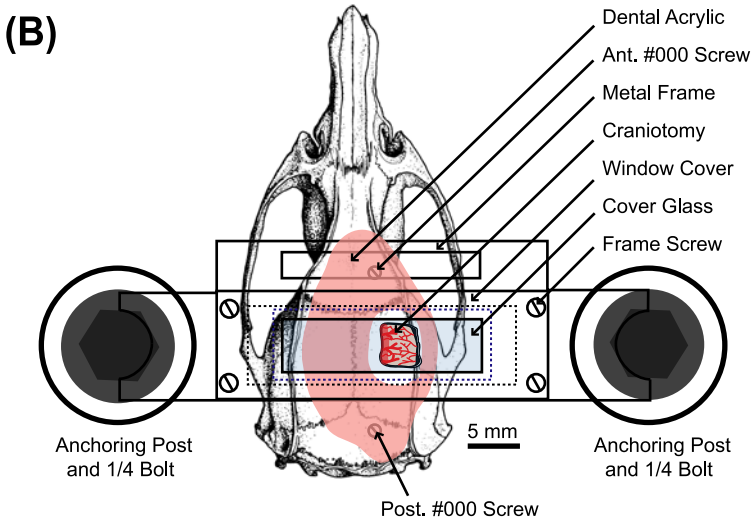

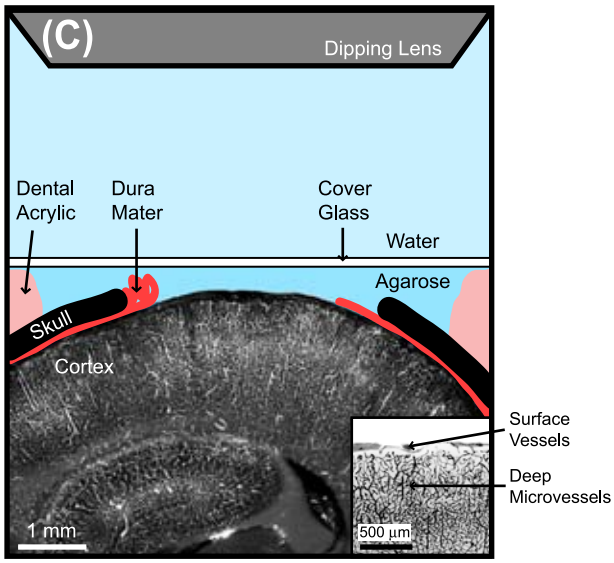

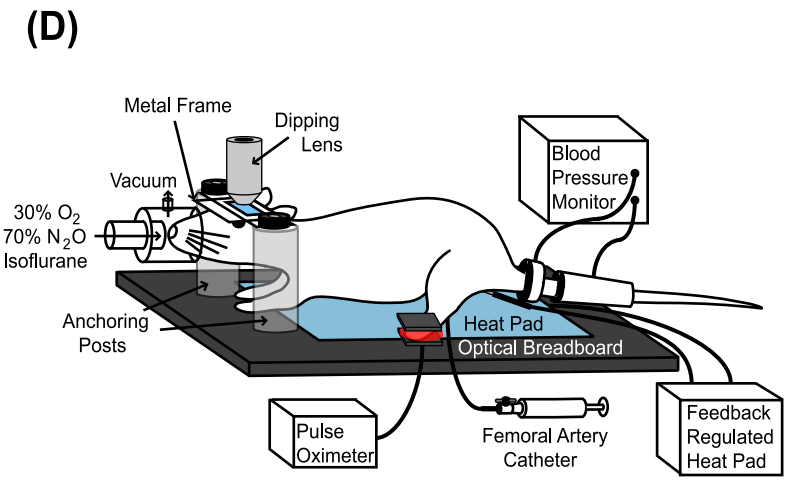

Figure 3. Kleinfeld, Friedman, Lyden and Shih

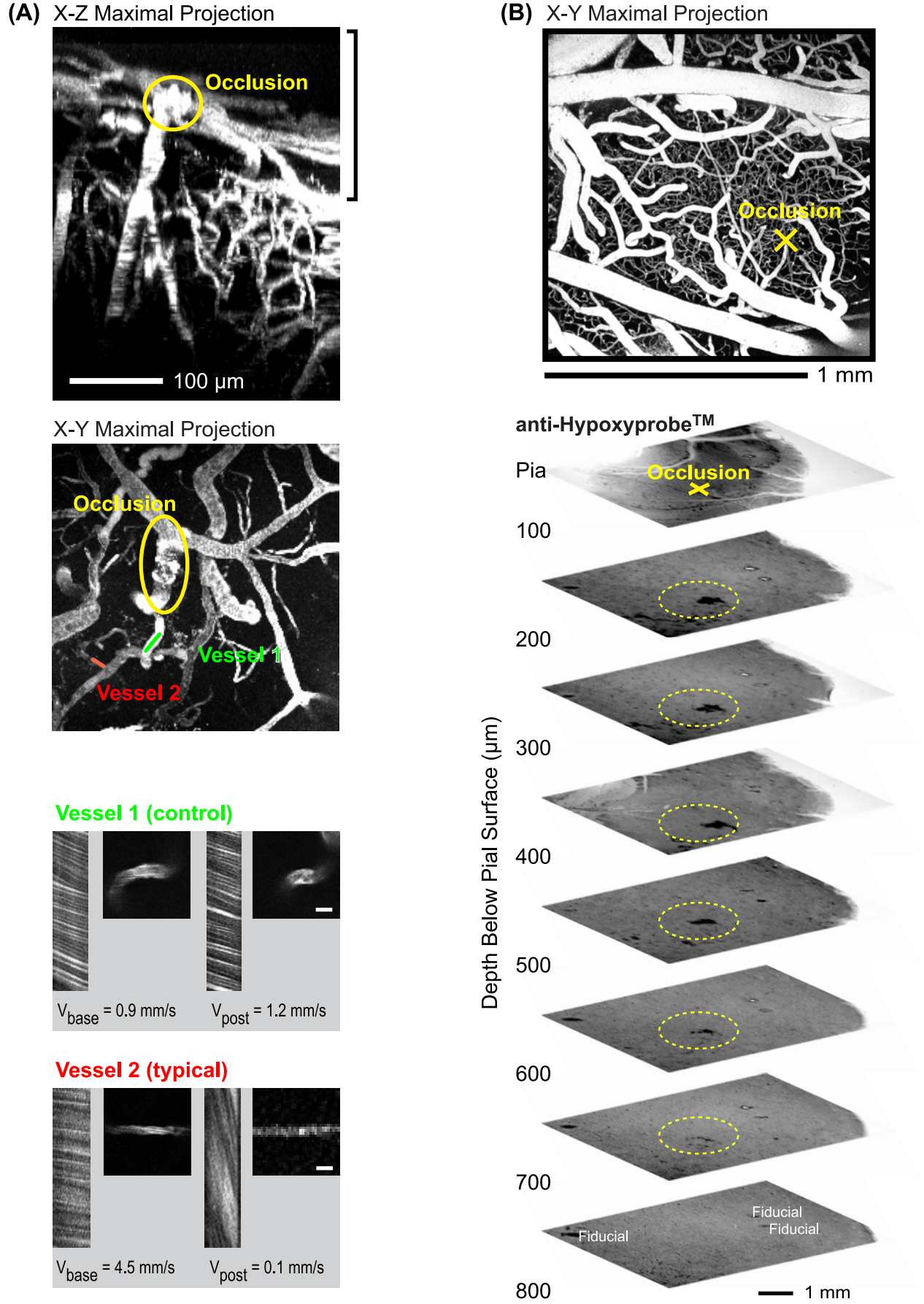

Figure 4. Kleinfeld, Friedman, Lyden and Shih

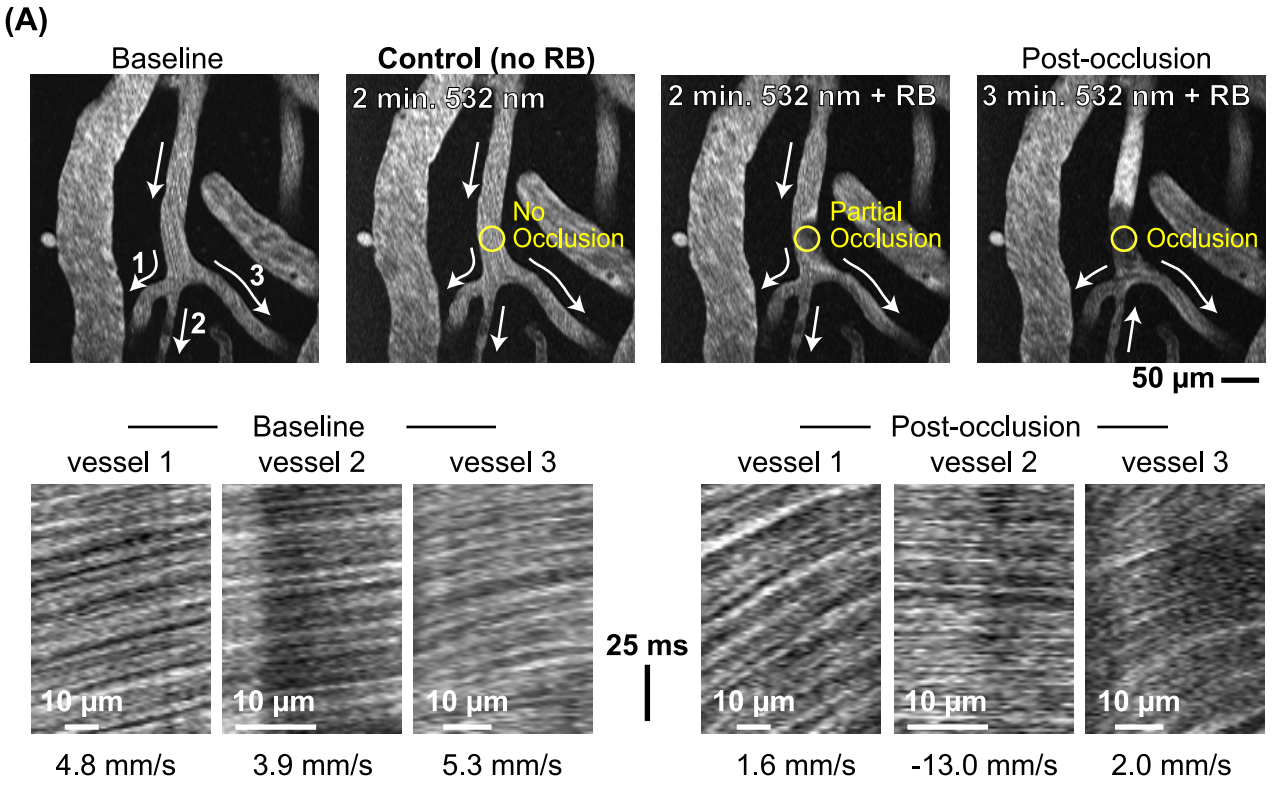

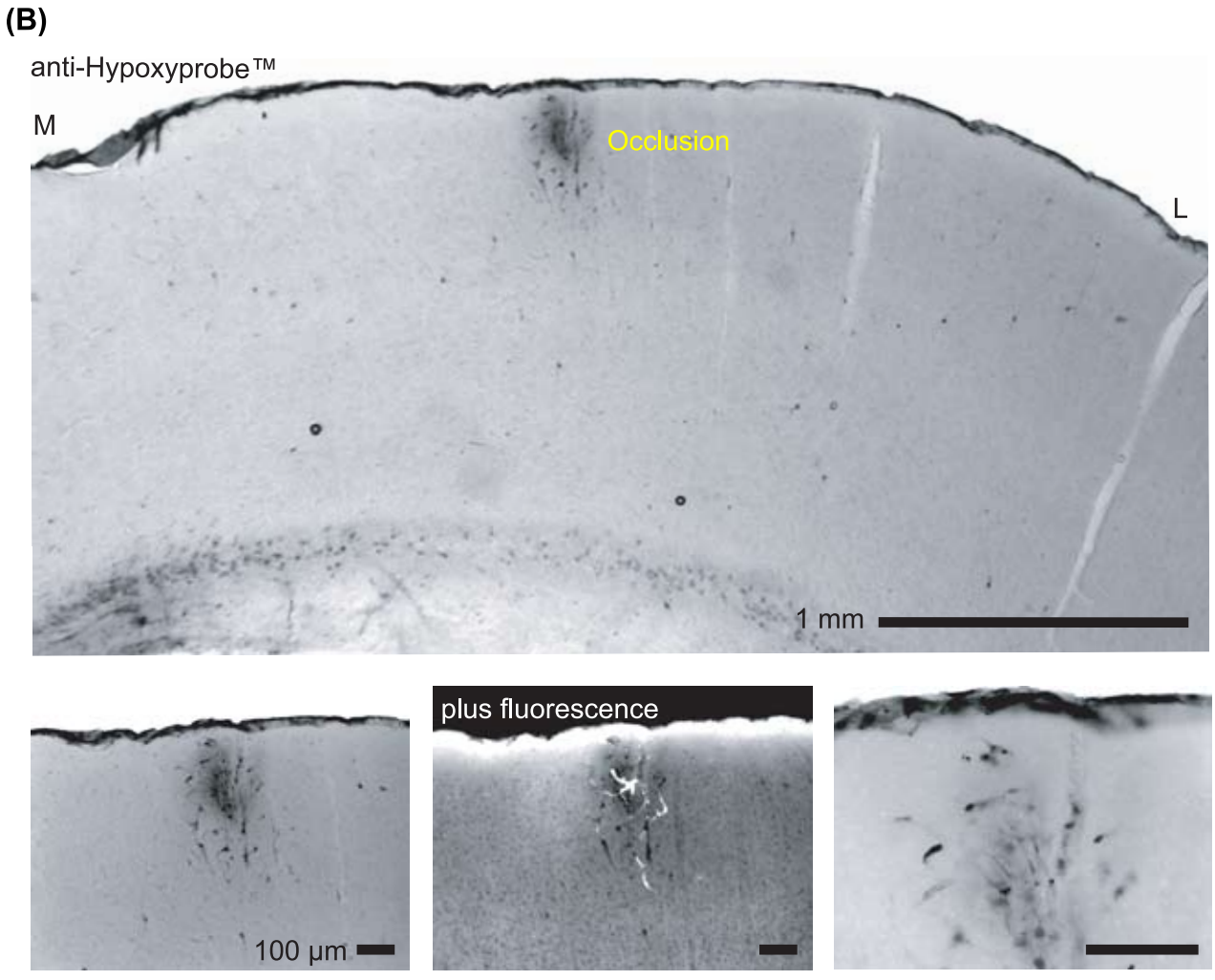

Figure 5. Kleinfeld, Friedman, Lyden and Shih

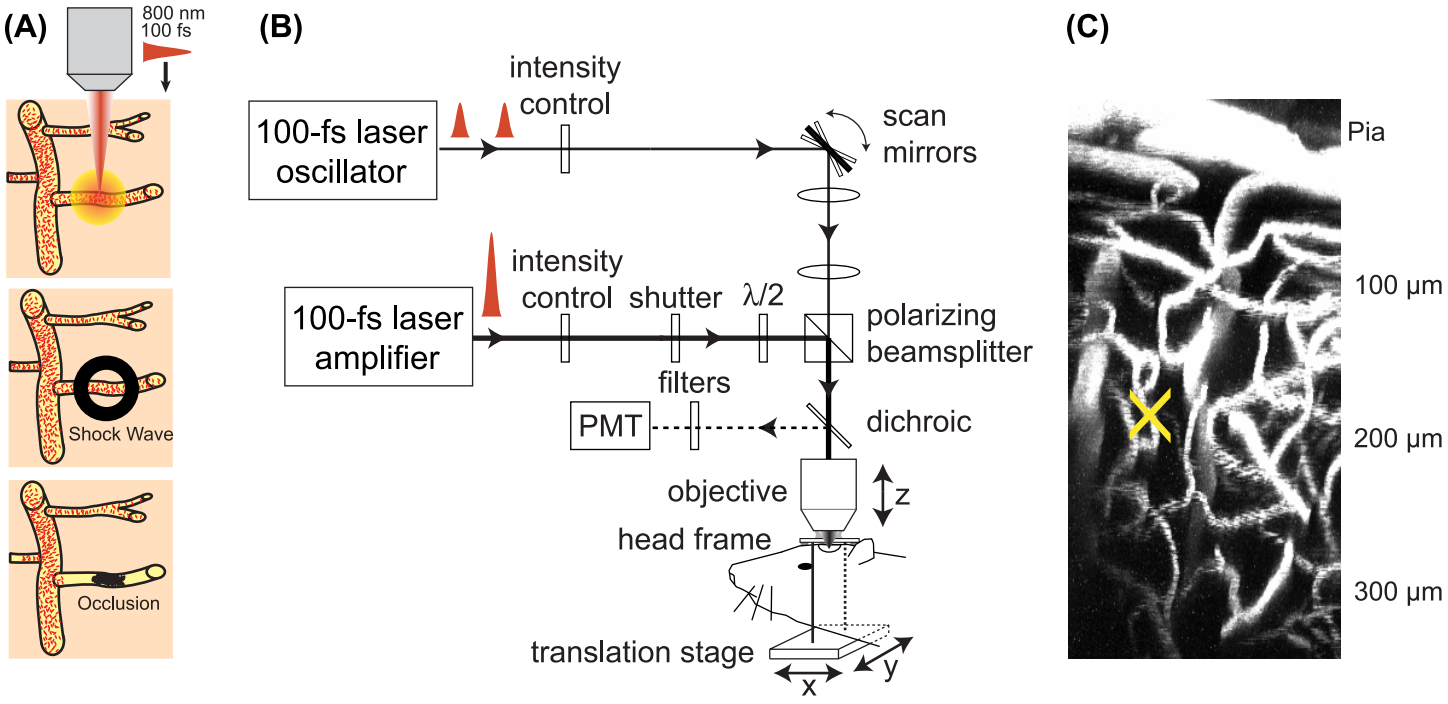

Figure 6. Kleinfeld, Friedman, Lyden and Shih

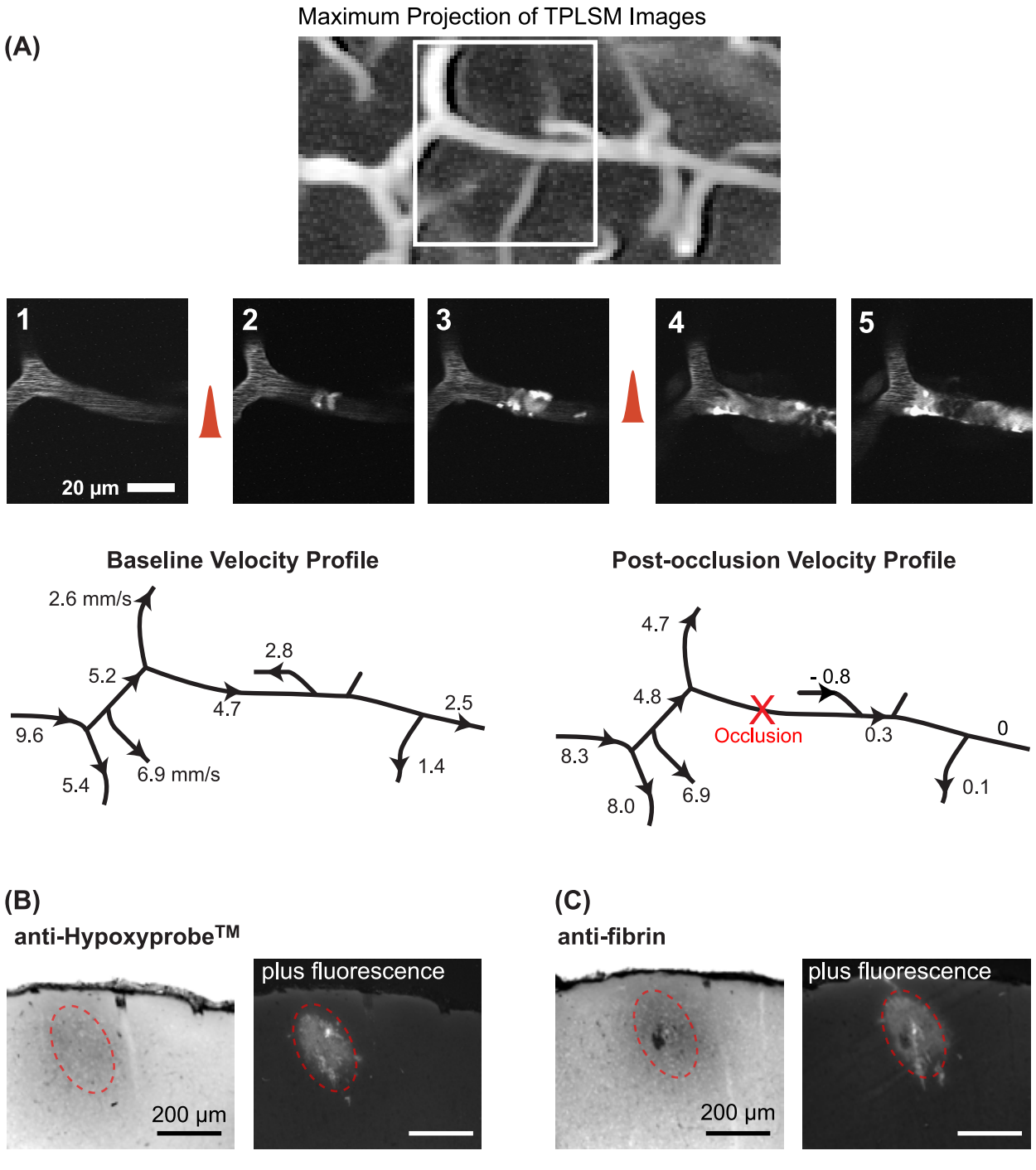

Figure 7. Kleinfeld, Friedman, Lyden and Shih